International Research Journal of Multidisciplinary Scope (IRJMS), 2026;7(3):1593-1605

Original Article | ISSN (O): 2582-631X DOI: 10.47857/irjms.2026.v07i03.010246

Analysis of Nanofluids in Tube Heat Exchanger

Murli Mukati*, Govind Maheshwari

Department of Mechanical Engineering, Institute of Engineering & Technology, DAVV, Indore, Madhya Pradesh, India. *Corresponding Author's Email: murliraj007@gmail.com

Abstract

The integration of nanotechnology offers a promising pathway to improve legacy heat-exchange systems by addressing the fundamental limitation of conventional fluids: their poor thermal conductivity. This experimental work examines the thermal and hydraulic behaviour of Copper-Water (Cu-W) and Graphene-Water (Gr-W) nanofluids in a horizontal tube-in-tube heat exchanger operated in the transitional turbulent range at a Reynolds number of about 4000. The nanofluids, stabilized using Sodium Lauryl Sulfate (SLS), were tested over a nanoparticle mass concentration range of 0-2.5 % and hot-fluid inlet temperatures between 60°C to 90 °C. The results show that increasing both nanoparticle concentration and operating temperature raises the overall heat transfer coefficient, U, and effectiveness, while Gr-W consistently delivers better thermal performance than Cu-W under identical test conditions. The thermal gains are accompanied by distinct hydraulic behaviour: Gr-W shows a monotonic increase in friction factor due to its higher effective viscosity, whereas Cu-W can exhibit a modest reduction in friction factor under the tested conditions, linked to the combined influence of density and viscosity on the Reynolds number at fixed volumetric flow rates. For both fluids, the counter-flow configuration outperforms parallel flow by maintaining a higher logarithmic mean temperature difference. Across all tested conditions, the PEC remains above unity, showing that the heat-transfer gain exceeds the corresponding pumping-power penalty. At 2.5 % mass concentration, the maximum PEC values of approximately 1.32 for Cu-W and 1.36 for Gr-W correspond to net efficiency gains of 32-36 % relative to the base fluid. Considering the measurement uncertainty, Gr-W nanofluid appears to be the more promising working fluid.

Keywords: Copper-Water (Cu-W), Graphene-Water (Gr-W), Heat Transfer Enhancement, Nanofluids, Performance Evaluation Criterion (PEC).

Introduction

The growing demand for energy-efficient thermal systems in power generation, automotive, and process industries has increased interest in advanced heat-transfer techniques and materials. Traditionally, water and ethylene glycol have been widely used as heat-transfer fluids in thermal systems, but their relatively low thermal conductivity restricts further gains in performance. Nanofluids are colloidal mixtures in which nanosized solid particles, usually in the 1–100 nm range, are dispersed within a base fluid such as water, oil, or ethylene glycol (1). Relative to conventional base fluids, nanofluids generally provide improved thermal performance because the suspended particles have higher conductivity, a larger surface area, and can induce micro-convection through Brownian motion (2). In practical operation, nanofluids may suffer from particle aggregation and settling, particularly because the particles are denser than the base fluid. Achieving long-term stability is therefore critical for obtaining reproducible experimental results. To improve dispersion stability, Sodium Lauryl Sulfate (SLS) was added as an anionic surfactant to generate electrostatic repulsion and suppress agglomeration. Figure 1 provides a visual check of the nanofluid stability after mixing, showing that no obvious phase separation was observed within the first 2 hours. Recent research in this area has placed considerable attention on metallic nanoparticles, particularly copper, owing to their high thermal conductivity and relatively low cost (3). For example, studies have reported that Cu-W nanofluids flowing through double-pipe heat exchangers can improve the Nusselt number and overall heat-transfer rate compared with water, primarily because copper nanoparticles increase the effective thermal conductivity and strengthen convective transport. However, metallic particles often have high density, which can lead to sedimentation and higher pumping-power penalties. In comparison, carbon-based nanomaterials such as graphene have emerged as a strong alternative because graphene nanosheets

(Received 23rd January 2026; Accepted 15th July 2026; Published 27th July 2026)

possess extremely high thermal conductivity and a high aspect ratio, which promote thermal percolation networks even at low concentrations. Graphene-based nanofluids have shown notable thermal gains in shell-and-tube exchangers while maintaining a much lower pressure-drop penalty than metal oxides (4). Graphene-based fluids exhibit superior thermal behaviour, particularly under turbulent flow conditions (5-7).

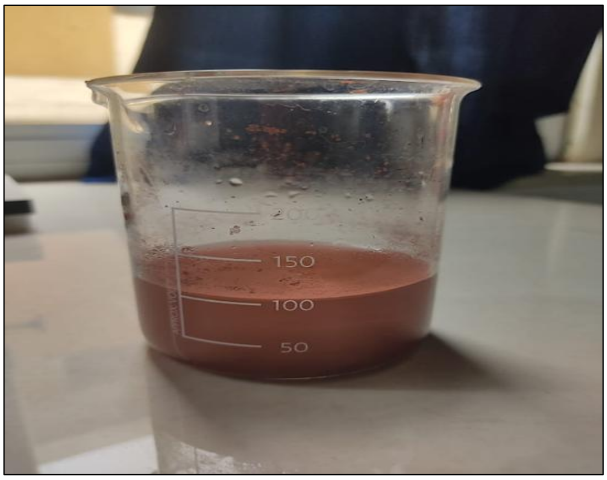

Figure 1: Visual Inspection of SLS-Stabilized Nanofluids After 2 Hours

The performance of different nanofluids in pipe-in-pipe and double-pipe heat exchangers has been thoroughly studied by many researchers. Metal-oxide fluids have been extensively studied for their thermal and flow characteristics (8, 9). Cu-W nanofluids have also attracted considerable attention because of their improved thermal performance (10, 11). More recently, hybrid and carbon-based nanofluids have gained interest for their potential energy-saving benefits (12, 13). In addition, the role of surfactants in improving nanofluid stability has been critically reviewed, and their influence on dispersion stability and thermophysical properties has been widely discussed (14, 15).

In recent years, both experimental and numerical investigations have explored graphene-based and hybrid nanofluids in double-pipe and shell-and-tube heat exchangers under practical operating conditions (16). For example, graphene nanoplatelet–water nanofluids have been tested in double-tube and concentric-tube heat exchangers, where adding nanoparticles led to notable increases in Nusselt number, overall heat-transfer coefficient, and effectiveness across wide Reynolds-number range (17, 18). Graphene oxide-based hybrid nanofluids combined with metallic nanoparticles have also been reported to improve the efficiency of double-pipe heat exchangers while keeping pressure drop and pumping-power requirements within acceptable limits (19, 20). Taken together, these studies highlight the strong promise of carbon-based nanofluids for compact heat-exchange systems (5, 13, 16).

However, even in these recent contributions, the focus is often limited to either a single nanofluid formulation or a single flow configuration, and the performance is usually expressed only in terms of local or average Nusselt numbers. System-level performance indicators that simultaneously account for heat-transfer enhancement and hydraulic penalties, such as the performance evaluation criterion (PEC), are less frequently reported, especially for graphene-based suspensions in conventional tube-in-tube geometries. There is still a need for systematic experimental data that compare a metal-based nanofluid such as Cu-W with a carbon-based counterpart such as Gr-W under identical hydrodynamic conditions, for both parallel- and counter-flow arrangements, and over a practical range of operating temperatures.

The present study addresses these gaps by experimentally investigating the thermophysical properties, thermal behaviour, and hydraulic performance of Cu-W and Gr-W nanofluids. The specific objectives of this study are:

a) To study the thermophysical behaviour of the nanofluids at mass concentrations up to 2.5%.
b) To analyse system performance using U , effectiveness, and NTU for both nanofluids under parallel and counter-flow arrangements.

c) To investigate the influence of operating temperature (60°C–90°C) on heat-transfer enhancement.
d) To perform a comparative efficiency analysis using the PEC to identify the optimal working fluid.

Methodology

Preparation of Nanofluids

In this study, Cu-W and Gr-W nanofluids were prepared using the conventional two-step approach. Copper and graphene nanoparticles were directly dispersed in water at mass concentrations from 0 to 2.5%, and the density of copper nanoparticles was taken as 8960 kg/m^3 based on standard material-property data and recent nanofluid studies. For graphene nanoparticles, the density value was considered as 2300 kg/m^3 according to manufacturer specifications and recent characterization studies (4, 5). Establishing a stable baseline for density and viscosity is essential for obtaining reliable thermal data, and the thermophysical properties were validated prior to testing following standard experimental protocols reported in the literature (21). This is consistent with broader findings that the high surface area of graphene contributes to improved energy efficiency and can exceed the thermodynamic performance of conventional metal oxides (22). For the copper-based samples, maintaining uniform dispersion remained a significant challenge, as minimizing sedimentation requires careful optimization of the dispersion process (23). Because strong Van der Waals forces tend to promote particle agglomeration, mechanical mixing alone is often inadequate. To improve dispersion stability, Sodium Lauryl Sulfate (SLS) was used as an anionic surfactant. For each nanofluid sample, SLS was added at the same mass percentage as the nanoparticles, corresponding to an approximate SLS-to-nanoparticle mass ratio of 1:1. This ratio was maintained for all Cu-W and Gr-W samples so that the surfactant effect remained comparable across the full test matrix. Separate measurements on SLS-water solutions without nanoparticles confirmed that, within this range, SLS introduced only a marginal change in the base fluid's viscosity and thermal conductivity of the base fluid; therefore, the dominant changes in thermophysical properties reported in this work can be attributed primarily to the nanoparticles rather than to the surfactant itself (24).

The mixtures were then ultrasonicated using an LC-650W ultrasonic homogenizer. Sonication time was varied between 20 and 60 minutes depending on mass concentration to ensure proper suspension quality. Visual inspection confirmed stable suspension with no visible sedimentation throughout the experimental period. Since the stability of the suspension directly influences heat transfer performance, a systematic characterization approach was adopted to ensure complete integration of the nano-additives into the base fluid (25).

Table 1: Thermophysical Properties of Copper, Graphene and Water

Property	Base Fluid (Water)	Copper (Cu)	Graphene (Gr)
Physical State	Liquid	Solid Powder	Solid Flakes
Density (ρ) (kg/m^3)	994.4	8960	2300
Thermal Conductivity (k) (W/m.K)	0.613	398	~4000
Specific Heat (c_p) (J/kg.K)	4180	385	710
Particle Size / Thickness	-	50–80 nm	5–10 nm

Table 1 presents the principal thermophysical properties of water and the nanoparticles used in this study. The substantially higher thermal conductivity of copper and graphene compared with water forms the basis for the expected improvement in heat transfer. In addition, differences in density and specific heat affect the effective properties of the resulting nanofluids. These variations are useful for interpreting the thermal and hydraulic trends discussed in the results section.

Experimental Apparatus

Figure 2 illustrates the complete experimental loop used for the heat-exchanger tests. It includes the heat exchanger, pump, storage tank, valves, and measuring instruments required for controlled operation. This setup enabled parallel-flow and counter-flow measurements under the same base conditions.

Figure 2: Photograph of the Experimental Setup

In this tube-in-tube heat exchanger, the tubes were installed horizontally and were made of stainless steel (SS). The heat exchanger was arranged in a double-tube configuration, with the inner tube having inner and outer diameters of 12 mm and 14 mm, respectively, and the outer tube having inner and outer diameters of 32 mm and 36 mm, respectively. The total tube length was 1000 mm.

To improve energy-balance accuracy, the entire length of the test section was clad with a thick layer of insulation to negate heat loss to the ambient environment. For experimental measurement, two calibrated rotameters were installed in the flow loop to measure the flow rates, while four thermocouples (K-type) were mounted at the respective inlet and outlet locations to continuously record the bulk fluid (T_{hi}, T_{ho}, T_{ci}, T_{co}).

Table 2: Experimental Operating Conditions

Parameter	Value / Range
Nanofluids	Cu-W, Gr-W
Base Fluid	Water
Surfactant	SLS
Mass Concentration (w)	0 %, 0.5 %, 1.0 %, 1.5 %, 2.0 %, 2.5 %
Hot Fluid Inlet Temp (T_{hi})	60 °C, 70 °C, 80 °C, 90 °C
Cold Fluid Inlet Temp (T_{ci})	21.8 ±0.5 °C
Reynolds Number (Re)	3900-4400 (Turbulent Transition)
Flow Arrangements	Parallel Flow, Counter Flow

Table 2 defines the operating window used for the experimental investigation. The selected Reynolds-number range was kept within the transitional turbulent regime to achieve a balance between heat-transfer enhancement and pumping-power requirement. The nanoparticle concentration ranges up to 2.5 % was chosen to study practical loading levels while maintaining suspension stability. Using an inlet temperature from 60°C to 90°C allows evaluation of the temperature sensitivity of both nanofluids under identical flow arrangements. The Reynolds number range of approximately 3900-4400 was selected intentionally to operate within the turbulent transition regime of the tube-in-tube heat exchanger. This range is practically relevant for compact industrial heat-exchange equipment, where designers aim to exploit the onset of turbulence to enhance heat transfer while avoiding the very high pumping-power penalties associated with fully developed turbulent flow.

Measurement of Thermophysical Properties

We focused this phase of the experiment on accurately quantifying the fluids' defining thermophysical traits, specifically measuring their density, viscosity, and thermal conductivity.

a) **Thermal Conductivity:** Measured using a digital conductivity meter.

b) **Viscosity:** Measured using a Brookfield viscometer.
c) **Density:** Determined using a standard **specific gravity bottle (pycnometer)** based on the relative density method, where the weight of the nanofluid was compared to that of an equal volume of water using a high-precision electronic balance.

Since the nanofluids were prepared based on mass concentration (w), these values were converted to volume fraction using Equation [1], which is based on the fundamental density relation reported in the literature (26).

$$\phi = \frac{\frac{w}{\rho_{np}}}{\frac{w}{\rho_{np}} + \frac{1-w}{\rho_{bf}}} \quad [1]$$

Here, w denotes the mass fraction, ρ_{np} denotes the nanoparticle density, and ρ_{bf} denotes the base-fluid density.

d) **Specific Heat:** In contrast to the transport properties, the specific heat capacity of the nanofluids ($C_{p,nf}$) was calculated using Equation [2]. This correlation is well established for dilute suspensions (19).

$$C_{p,nf} = \phi C_{p,np} + (1-\phi) C_{p,bf} \quad [2]$$

Where, $C_{p,np}$ and $C_{p,bf}$ denotes the specific heat capacities of the nanoparticles and the base fluid, respectively.

Data Reduction

The performance of the heat exchanger, in terms of heat transfer and hydraulics, was determined using the relations below.

Flow Velocity and Mass Flow Rate

The thermal and hydraulic performance of the heat exchanger was assessed using the heat-transfer rate (Q), the overall heat transfer coefficient (U), and the dimensionless parameters Re and Pr (27).

The calculation process began by determining the mass flow rate ($\dot{m}$) from the measured volumetric flow rate ($\dot{V}$) and fluid density using Equation [3]:

$$\dot{m} = \rho \times \dot{V} \quad [3]$$

The mean flow velocities for both fluids were obtained using Equations [4, 5].

Cold Fluid Velocity (V_c):

$$V_c = \frac{\dot{V}_c}{A_{cs,i}} = \frac{\dot{V}_c}{\frac{\pi}{4} d_i^2} \quad [4]$$

Hot Fluid Velocity (V_h):

$$V_h = \frac{\dot{V}_h}{A_{cs,o}} = \frac{\dot{V}_h}{\frac{\pi}{4}(D_i^2 - d_o^2)} \quad [5]$$

Here, d_i and d_o denote the inside and outside diameters of the inner tube, respectively, whereas D_i denotes the inner diameter of the outer shell.

Heat Transfer Parameters

The rate of heat transfer for the hot and cold streams was determined using the energy balance Equations [6, 7]:

$$Q_h = \dot{m}_h C_{p,h} (T_{h,in} - T_{h,out}) \quad [6]$$

$$Q_c = \dot{m}_c C_{p,c} (T_{c,out} - T_{c,in}) \quad [7]$$

The average rate of heat transfer was denoted in Equation [8],

$$Q_{avg} = (Q_h + Q_c)/2 \quad [8]$$

Using these values, the experimental overall heat transfer coefficient (U) was obtained using Equation [9]:

$$U = \frac{Q_{avg}}{A_i \times \Delta T_{LMTD}} \quad [9]$$

The effective driving temperature difference, represented by ΔT_{LMTD}, for counter-flow and parallel-flow arrangements, was calculated using Equations [10, 11].

For Counter Flow:

$$\Delta T_{LMTD} = \frac{(T_{h,in}-T_{c,out})-(T_{h,out}-T_{c,in})}{\ln\left(\frac{T_{h,in}-T_{c,out}}{T_{h,out}-T_{c,in}}\right)} \quad [10]$$

For Parallel Flow:

$$\Delta T_{LMTD} = \frac{(T_{h,in}-T_{c,in})-(T_{h,out}-T_{c,out})}{\ln\left(\frac{T_{h,in}-T_{c,in}}{T_{h,out}-T_{c,out}}\right)} \quad [11]$$

Dimensionless Numbers and Validation

The flow characteristics were analysed by calculating the Reynolds and Prandtl numbers from the bulk mean properties using Equations [12, 13]. Thermal conductivity, density, specific heat, and viscosity were obtained from standard property tables, while the governing expressions were used in the form given in another study (27).

$$Re = \frac{\rho VD}{\mu} \quad [12]$$

$$Pr = \frac{\mu c_p}{k} \quad [13]$$

For experimental validation, the theoretical Nusselt number for the base fluid (water) was calculated using Equation [14], based on Dittus-Boelter correlation (28).

$$Nu_{th} = 0.023Re^{0.8}Pr^{0.4} \quad [14]$$

Using the inner convective heat-transfer coefficient (h_i), the experimental Nusselt number (Nu_{exp}) was determined using Equation [15]:

$$Nu_{exp} = \frac{h_i d_i}{k_{nf}} \quad [15]$$

Effectiveness-NTU Method

Heat-exchanger effectiveness was assessed using the NTU method, and the equations for both parallel-flow and counter-flow arrangements were taken from established literature sources (29).

The effectiveness was then calculated using the NTU approach. First, the heat-capacity rates ($C = \dot{m}c_p$) computed to determine C_{min} and C_{max}, and the capacity ratio was obtained by Equation [16].

$$C_r = C_{min}/C_{max} \quad [16]$$

The NTU was calculated using Equation [17]:

$$NTU = \frac{U \times A_i}{C_{min}} \quad [17]$$

Heat-exchanger effectiveness was evaluated using the NTU method, and the expressions for counter-flow and parallel-flow arrangements wer4e applied from Equations [18, 19], respectively.

For Counter Flow:

$$\epsilon = \frac{1-\exp(-NTU(1-C_r))}{1-C_r\exp(-NTU(1-C_r))} \quad [18]$$

For Parallel Flow:

$$\epsilon = \frac{1-\exp(-NTU(1+C_r))}{1+C_r} \quad [19]$$

Hydraulic and Performance Evaluation

The hydraulic penalty was evaluated using the friction factor (f) using Equation [20]. The Blasius equation was used for turbulent flow transition regime (30).

$$f = 0.3164\ Re^{-0.25} \quad [20]$$

Finally, to assess the net energy efficiency, the performance evaluation criterion (PEC) was calculated using Equation [21], as given in past study (31).

$$PEC = \frac{(U_{nf}/U_{bf})}{(f_{nf}/f_{bf})^{1/3}} \qquad [21]$$

Table 3: Specifications and Uncertainty of Experimental Instruments

Parameter Measured	Instrument	Range	Accuracy / Uncertainty
Temperature	K-Type Thermocouples	0 – 200 °C	± 0.1 °C
Flow Rate	Rotameter	0 – 10 LPM	± 2 %
Viscosity	Brookfield Viscometer	1 – 100 mPa.s	± 1 %
Thermal Conductivity	Conductivity Meter	0.2 – 2.0 W/m.K	± 5 %
Weight (Mass)	Digital Electronic Balance	0 – 200 g	± 0.001 g

Uncertainty Analysis

Table 3 lists the major instruments used for temperature, flow rate, viscosity, thermal conductivity, and mass measurement. The selected devices were sufficiently accurate for the present low-temperature-gradient experiments. Their uncertainties directly affected the reliability of the energy-balance check, thermophysical-property measurement, and performance calculations. This instrument summary supports the uncertainty analysis reported in the methodology section.

The uncertainty levels were assigned according to the measured quantity: 5 % for the energy-balance validation line ($Q_h = Q_c$), up to 5 % for thermal conductivity, below 1 % for viscosity, and 3% for effectiveness and friction factor.

Stability and Repeatability

In addition to the initial visual inspections shown in Figure 1, the nanofluid samples were monitored over the full experimental period for signs of sedimentation or phase separation.

No visible settling was observed within the time window corresponding to a complete set of heat-transfer measurements for a given test condition. Each operating point reported in this work represents the average of three repeated runs performed after a fresh mixing cycle. The maximum deviation between the three repeats was typically 3-6 % for both the overall heat transfer coefficient and the friction factor. Because in-house zeta-potential facilities were unavailable, the stability assessment was limited to these extended visual observations and repeatability checks; future work will incorporate quantitative electro-kinetic characterisation to strengthen the stability analysis.

Results and Discussion

Validation of Experimental Setup

To verify the experimental system, water was first used as the working fluid, and an energy-balance comparison was made between the heat rejected by the hot fluid (Q_h) and the heat absorbed by the cold fluid (Q_c) over the full temperature range.

Figure 3 shows that the experimental data points lie reasonably close to the ideal diagonal line ($Q_h = Q_c$). A consistent and nearly uniform trend is observed, as expected, and the calculated Q_c values were marginally lower than Q_h because of minor thermal leakage despite the insulation. Overall, the average energy-balance deviation remained within permissible limits and was consistent with uncertainties reported in similar low-temperature-gradient studies. This agreement supports the reliability of the thermocouple readings and flow measurements before testing the nanofluids.

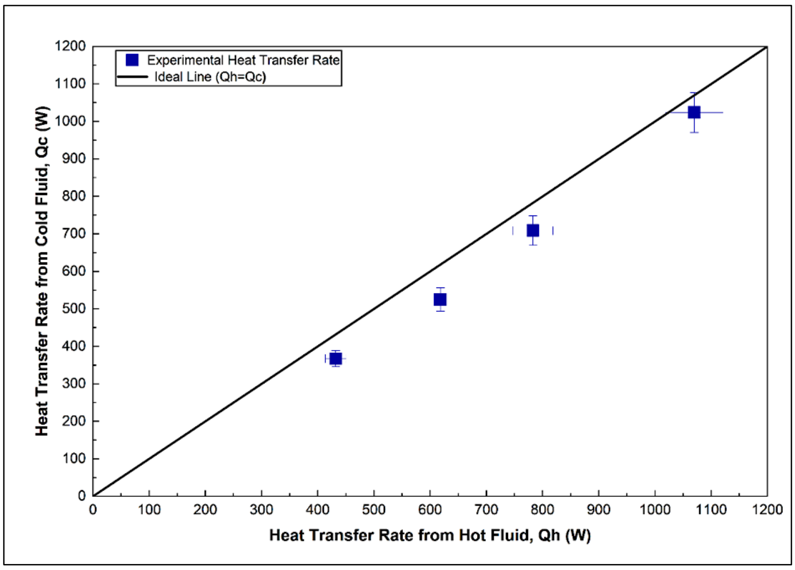

Figure 3: Energy-Balance Validation of Heat Transfer Rates with Experimental Uncertainty Bars

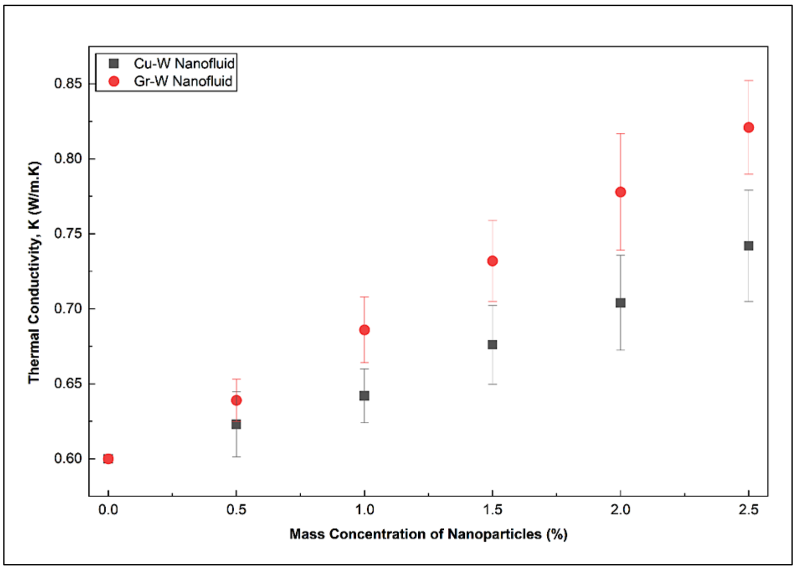

Figure 4: Thermal Conductivity of Cu-W and Gr-W Nanofluids with Experimental Uncertainty Bars

Thermophysical Properties of Nanofluids

Thermal Conductivity

Thermal conductivity is an essential parameter in judging the heat-transfer potential of the working fluid.

Figure 4 shows the experimental thermal-conductivity trends for both Cu-W and Gr-W nanofluids. The results indicate that incorporating nanoparticles increases conductivity relative to the base fluid. This enhancement is linked to the high thermal conductivity of the dispersed phase and the formation of an ordered nanolayer at the solid–liquid interface, which together facilitate heat transfer (14).

The Gr-W nanofluid exhibited higher conductivity than the Cu-W nanofluid over the tested concentration range, with the maximum value obtained at 2.5% graphene concentration. The error bars in the figure represent the estimated experimental uncertainty associated with each measurement. The observed difference is mainly due to the much higher conductivity of graphene compared with copper, along with the large surface area of the 2D graphene structure, which favours stronger surface interaction and more effective thermal-network formation in the base fluid.

Viscosity

Even though nanoparticles improve thermal conductivity, the viscosity increase controls the pumping power needed during operation.

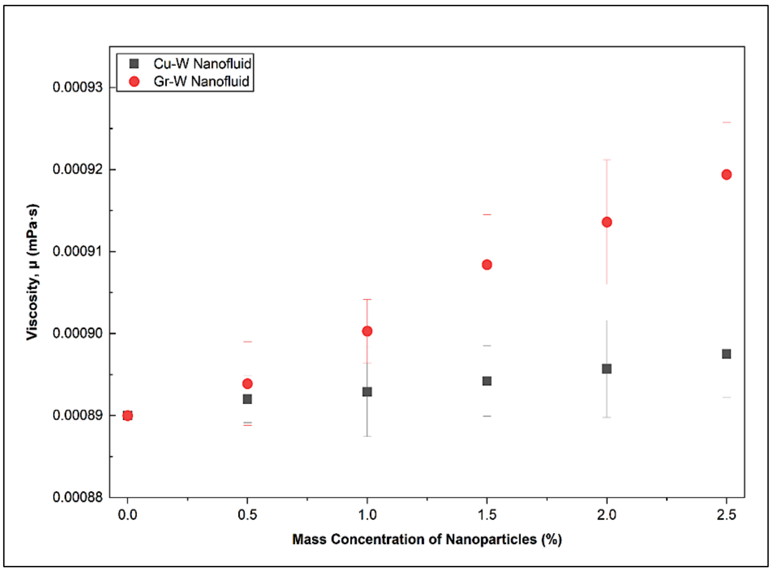

Figure 5: Dynamic Viscosity of Cu-W and Gr-W Nanofluids with Experimental Uncertainty Bars

Figure 5 shows measured viscosity increased with increasing nanoparticle mass concentration for both nanofluids. However, the Gr-W nanofluid showed a steeper increase than the Cu-W nanofluid. This behaviour is consistent with rheological studies, where the high-aspect-ratio planar structure of graphene sheets produces higher hydrodynamic resistance than relatively spherical copper nanoparticles (16). Even with these increases, the viscosity values across all tested concentrations remained within feasible pumping limits.

Effectiveness

The effectiveness was used as the primary performance metric to evaluate how the Cu-W and Gr-W nanofluids responded to the change from parallel flow to counter-flow.

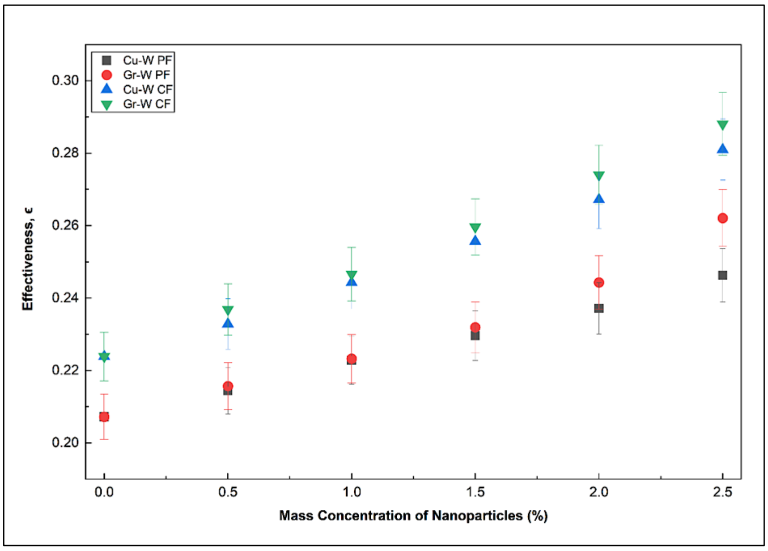

Figure 6: Effectiveness of Cu-W and Gr-W Nanofluids under Parallel and Counter Flow with ±3% Uncertainty Bars

Figure 6 shows a consistent increase in effectiveness with nanoparticle concentration for both fluids, which can be linked to improved thermal conductivity and intensified wall heat transfer. The distinct advantage of graphene over copper in our tests mirrors the recent exergy analysis, which showed that graphene-based blends typically generate less entropy and outperform standard oxides like CuO and Al_2O_3 (32).

The results also show that the counter-flow arrangement consistently produced higher effectiveness than the parallel-flow configuration at all concentrations.

This is in line with conventional heat-exchanger behaviour, as counter-flow arrangement maintains a stronger temperature gradient throughout the exchanger length. At the maximum tested loading of 2.5%, the Gr-W suspension gave the highest effectiveness, about 0.28, which was higher than that of the Cu-W nanofluid under the same conditions.

Operating Temperature

The effect of temperature on heat-exchanger performance was assessed by comparing the overall heat-transfer coefficient (U) at different hot-fluid inlet temperatures for the 2.5% nanofluids.

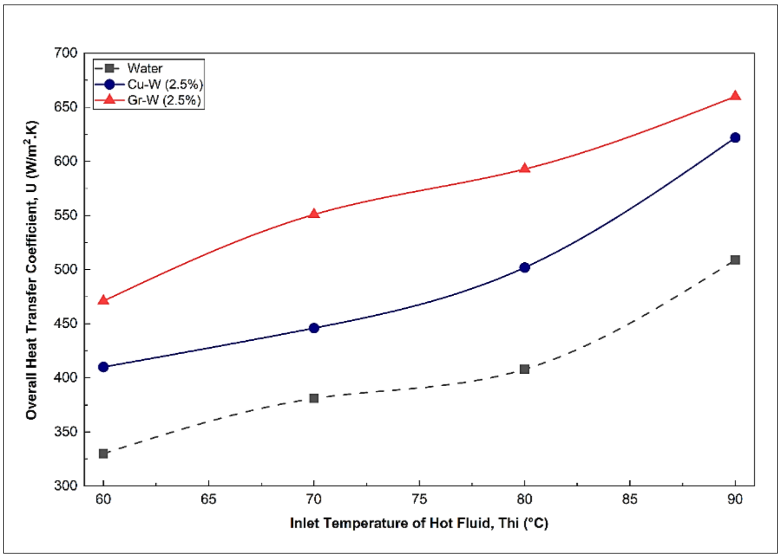

Figure 7: Overall Variation of Overall Heat-Transfer Coefficient for Water and Nanofluids at Different Inlet Temperatures

Figure **7** shows that the overall heat-transfer coefficient increased with hot-fluid temperature for all tested fluids. For the Gr-W nanofluid, it rose from 471 W/m^2K at 60°C to 660 W/m^2K at 90°C. This trend can be explained by two main effects: lower viscosity at higher temperatures, which reduces the thermal boundary-layer resistance near the wall, and stronger Brownian motion of the nanoparticles, which enhances microscale convective transport (2, 17).

Hydraulic Characteristics (Friction Factor)

The addition of nanoparticles improved heat transfer but also introduced a hydraulic penalty through viscous drag. The friction factor (f) was evaluated using the Blasius correlation (30).

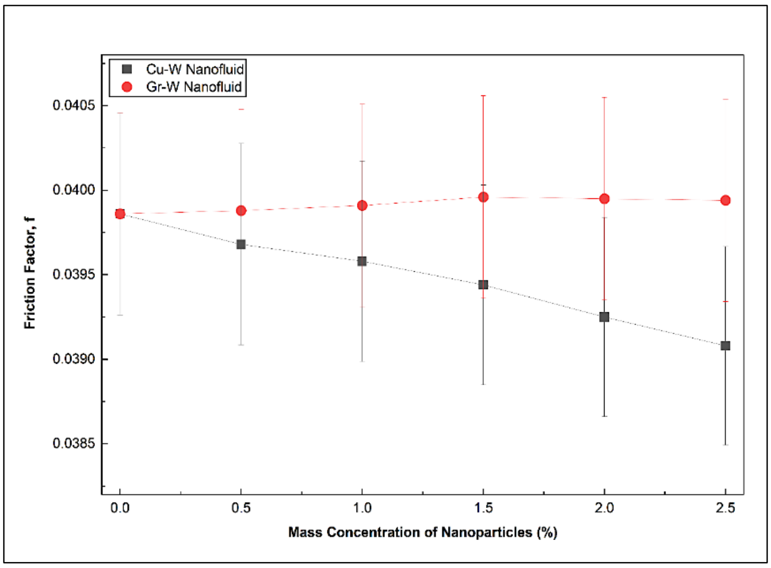

Figure 8: Friction Factor of Cu-W and Gr-W Nanofluids

The above Figure 8 indicates different hydraulic characteristics of the two nanofluids. For the Gr-W nanofluid, the friction factor increased gradually with concentration, which is the expected trend because of the viscosity penalty associated with graphene sheets (33).

The Cu-W nanofluid showed a different trend: the friction factor decreased slightly with increasing concentration under the tested conditions. The observed behaviour results from the combined influence of higher density and lower viscosity, leading to a larger Reynolds number for a given volumetric flow rate. According to the Blasius correlation, a higher Reynolds number corresponds to a lower friction factor. Similar density-dominated behaviour has also been reported for metal-based nanofluids in turbulent flow (20, 34).

System Performance Evaluation Criterion (PEC)

Since the performance evaluation criterion was above unity over the whole operating range, the thermal improvement was greater than the associated pumping-power penalty.

Figure 9 compares the performance evaluation criterion (PEC) of Cu-W and Gr-W nanofluids across the tested concentration range.

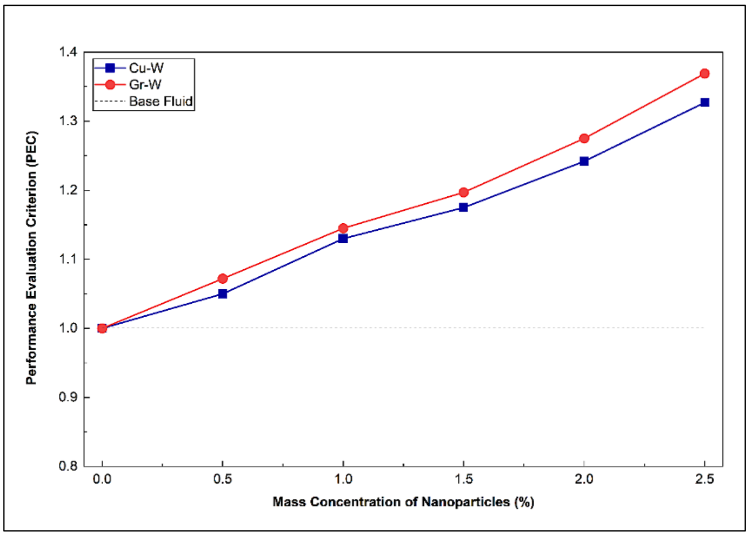

Figure 9: PEC of Cu-W and Gr-W Nanofluids with Nanoparticle Concentration

Figure 9 shows that nearly identical PEC values were observed at 1% concentration, where the performance of the two nanofluids converged. Beyond 1% concentration, the Gr-W nanofluid showed the stronger thermal enhancement, despite its higher viscosity. The highest PEC values were obtained at 2.5% mass concentration, with approximately 1.32 for Cu-W and 1.36 for Gr-W. These values correspond to net efficiency gains of about 32% and 36%, respectively, relative to the base fluid. Considering the experimental uncertainty, the small difference between these two values should be interpreted cautiously, but the overall trend indicates that graphene-based nanofluids provided equal or slightly better performance than copper-based nanofluids.

Conclusion

This study experimentally examined the thermal and hydraulic performance of Cu-W and Gr-W nanofluids in a turbulent double-tube heat exchanger operated under both parallel-flow and counter-flow conditions. The results indicate that increasing nanoparticle concentration up to 2.5% enhanced thermal conductivity, overall heat-transfer coefficient, effectiveness, and PEC for both nanofluids, although it also caused a rise in viscosity.

Gr-W consistently showed better thermal performance than Cu-W, especially at higher concentrations, because of its higher intrinsic thermal conductivity and favourable particle morphology. In every case, the counter-flow arrangement performed better than the parallel-flow setup, demonstrating the benefit of sustaining a larger temperature driving force along the exchanger length.

In the case of Gr-W, the overall heat-transfer coefficient rose from 471 W/m^2K at 60°C to 660 W/m^2K at 90°C, demonstrating that elevated operating temperature enhances heat-transfer performance. The PEC remained above unity throughout the study, indicating that the heat-transfer improvement outweighed the associated hydraulic penalty.

At the maximum concentration of 2.5%, the PEC values reached approximately 1.32 for Cu-W and 1.36 for Gr-W, suggesting that both nanofluids are energetically viable, with Gr-W providing a slight performance advantage. Overall, the results indicate that 2.5% Gr-W in counter-flow mode is the most favourable condition among the tested cases for compact heat-exchanger applications.

Abbreviations

ϵ: Effectiveness, ϕ: Volume fraction, f: Friction factor, LMTD: Logarithmic Mean Temperature Difference, $\dot{m}$: Mass flow rate, NTU: Number of Transfer Units, Q: Heat transfer rate, U: Overall heat transfer coefficient, $\dot{V}$: Volumetric flow rate, w: Mass concentration of nanoparticles.

Acknowledgement

The authors gratefully acknowledge the Department of Mechanical Engineering, IET-DAVV, Indore, for providing access to the laboratory facilities and technical support during this experimental work.

Author Contributions

Murli Mukati: Conceptualization, Experimental Design, Data Acquisition, Data Curation, Formal Analysis, Preparation of the Original Draft, Govind Maheshwari: Supervision, Methodological Refinement, Result Interpretation, Critical Review of the Manuscript, Approved the Final Version. Both authors approved the manuscript for submission.

Conflict Of Interest

The authors declare no competing financial or personal interests that could have affected the work reported in this manuscript.

Data Availability

The datasets generated and analysed during the current study are available from the corresponding author on reasonable request.

Declaration of Artificial Intelligence (AI) Assistance

The authors used generative AI tools only for language refinement and grammatical editing. The research ideas, experimental data, analysis, and conclusions are entirely original to the authors.

Ethics Approval

Not applicable. This study involved experimental analysis of mechanical systems and did not involve human participants or animals.

Funding

The authors received no specific funding from any public, commercial, or not-for-profit agency for this study.

References

1. Yu W, Xie H. A review on nanofluids: preparation, stability mechanisms, and applications. J Nanomater. 2012; 2012:435873. doi:10.1155/2012/435873
2. Buongiorno J. Convective transport in nanofluids. J Heat Transfer. 2006;128(3):240-250. doi:10.1115/1.2150834
3. Sokhal GS, Gangacharyulu D, Bulasara VK. Effectiveness and thermal performance analysis of copper nanofluids flow in a U-bend double-pipe heat exchanger. Heat Transf Res. 2021;52(1):31-59. doi:10.1615/HeatTransRes.2020034397
4. Zolfalizadeh M, Zeinali Heris S, Pourpasha H, Mohammadpourfard M, Meyer JP. Experimental investigation of the effect of graphene/water nanofluid on the heat transfer of a shell-and-tube heat exchanger. Int J Energy Res. 2023:2023;3477673. doi:10.1155/2023/3477673
5. Arshad A, Jabbal M, Yan Y, Reay D. Graphene nanoplatelets nanofluids in thermal management applications: A comprehensive review. Therm Sci Eng Prog. 2020;18:100518. doi: 10.1016/j.tsep.2020.100518
6. Patel BV, Sarviya RM, Rajput SPS. Improving hydrothermal performance of a tubular heat exchanger with different types of twisted tapes using graphene nanoplatelets/water nanofluid. Energy Sources A Recover Util Environ Eff. 2023:12695-710. doi:10.1080/15567036.2023.2276383
7. Shibata A, Fujimoto K, Torii S. Heat transfer enhancement of graphene nanofluid manufactured from graphite sheet. Mater Today Proc. 2022;66(2):809-814. doi: 10.1016/j.matpr.2022.05.288
8. Duangthongsuk W, Wongwises S. Heat transfer enhancement and pressure drop characteristics of TiO2-water nanofluid in a double-tube counter flow heat exchanger. Int J Heat Mass Transf. 2009;52(7-8):2059-2067. doi: 10.1016/j.ijheatmasstransfer.2008.10.023
9. Suganthi KS, Rajan KS. Metal oxide nanofluids: review of formulation, thermo-physical properties, mechanisms, and heat transfer performance. Renew Sustain Energy Rev. 2017; 76:226-255. doi: 10.1016/j.rser.2017.03.043
10. Aligholami M, Akbari M, Maaza M. Thermal performance of copper-distilled water nanofluid in a wavy channel. Mater Today Proc. 2023. doi: 10.1016/j.matpr.2023.07.373
11. Shaik AH, Chakraborty S, Saboor S, *et al*. Cu-graphene water-based hybrid nanofluids: synthesis, stability,

thermophysical characterization, and figure of merit analysis. J Therm Anal Calorim. 2024;149:2953-2968.
doi:10.1007/s10973-023-12875-x

12. Das PK, Santra AK, Ganguly R, Dash SK. An extensive review of preparation, stabilization, and application of single and hybrid nanofluids. J Therm Anal Calorim. 2024;149:9523-9557.
doi:10.1007/s10973-024-13449-1
13. Borode AB, Tshephe T, Olubambi PO. A critical review of the thermophysical properties and applications of carbon-based hybrid nanofluids in solar thermal systems. Front Energy Res. 2025;12:1509437.
doi:10.3389/fenrg.2024.1509437
14. Wang J, Yang X, Klemeš JJ, Tian K, Ma T, Sundén B. A review on nanofluid stability: preparation and application. Renew Sustain Energy Rev. 2023; 188:113854.
doi: 10.1016/j.rser.2023.113854
15. Purree S, Nadeem M, Shahzad A, Ali HM. Synthesis, heat transfer properties and stability of nanofluids for commercialization: A review. Chem Eng Commun. 2023;210(5):814-836.
doi:10.1080/00986445.2021.1976163
16. Patel P, Pathak R. Experimental analysis and comparison of thermophysical properties of the three different hybrid nano-catalyst blended diesel fuels. Aust J Mech Eng. 2025;23(3):628-43. doi:10.1080/14484846.2023.2205566
17. Zolfalizadeh M, Heris SZ, Pourpasha H, Mohammadpourfard M, Meyer JP. Experimental investigation of the effect of graphene/water nanofluid on the heat transfer of a shell-and-tube heat exchanger. Int J Energy Res. 2023;2023:3477673.
doi:10.1155/2023/3477673
18. Shrotriya A, Nayak C, Sahu NK. Dispersion properties evaluation of copper-based nanoparticles as cutting fluid using Taguchi-based grey relational analysis. J Eng Appl Sci. 2025;72:82.
doi:10.1186/s44147-025-00649-1
19. Shrotriya A, Vakharia V, Borade H, Chaudhari R, Vora J. An ensemble learning approach for predicting nanoparticle dispersion properties in cutting fluids using a small sample dataset. Int J Thermofluids. 2025;27:101262.
doi: 10.1016/j.ijft.2025.101262
20. Patel P, Pathak R, Shukla AK. Experimental analysis of thermophysical properties of the nano-catalyst blended diesel fuel. In: Scientific and Technological Advances in Materials for Energy Storage and Conversions. Singapore: Springer Nature; 2023. p.109-26.
doi:10.1007/978-981-97-2481-9_9
21. Sujith SV, Kim H, Lee J. A review on thermophysical property assessment of metal oxide-based nanofluids: Industrial perspectives. Metals. 2022;12(1):165.
doi:10.3390/met12010165
22. Armstrong M, Mahadevan S, Selvapalam N, *et al.* Augmenting the double pipe heat exchanger efficiency using varied molar Ag ornamented graphene oxide nanoparticles aqueous hybrid nanofluids. Front Mater. 2023;10:1240606.
doi:10.3389/fmats.2023.1240606
23. Incropera FP, DeWitt DP, Bergman TL, Lavine AS. Fundamentals of Heat and Mass Transfer. 7th ed. New York: John Wiley & Sons; 2011.
https://books.google.com/books?id=vvyIoXEywMoC
24. Dittus FW, Boelter LMK. Heat transfer in automobile radiators of the tubular type. Int Commun Heat Mass Transf. 1985;12:3-22.
doi:10.1016/0735-1933(85)90003-X
25. Kays WM, London AL. Compact Heat Exchangers. 3rd ed. New York: McGraw-Hill; 1984.
https://www.osti.gov/biblio/6132549
26. Yadav D, Nirala A, Kumar R, Singh PK. Density variation in nanofluids as a function of concentration and temperature. Mater Today Proc. 2021;46(15):6576-80.
doi: 10.1016/j.matpr.2021.04.052
27. Khanafer K, Vafai K. A critical synthesis of thermophysical characteristics of nanofluids. Int J Heat Mass Transf. 2011;54(19-20):4410-28.
doi: 10.1016/j.ijheatmasstransfer.2011.04.048
28. Dittus FW, Boelter LMK. Heat transfer in automobile radiators of the tubular type. Int Commun Heat Mass Transf. 1985;12:3-22.
doi:10.1016/0735-1933(85)90003-X
29. El-Maghlany WM, Hanafy AA, Hassan AA, El-Magid MA. Experimental study of Cu-water nanofluid heat transfer and pressure drop in a horizontal double-tube heat exchanger. Exp Therm Fluid Sci. 2016;78:100-11.
doi: 10.1016/j.expthermflusci.2016.05.015
30. White FM. Fluid Mechanics. 8th ed. New York: McGraw-Hill Education; 2016.
https://books.google.co.in/books/about/Fluid_MecMechan.html?id=NqpZCgAAQBAJ&redir_esc=y
31. Sundar LS, Singh MK, Sousa ACM. Turbulent heat transfer and friction factor of graphene oxide/water nanofluids in a circular tube. Int Commun Heat Mass Transf. 2023;145:106822.
doi: 10.1016/j.icheatmasstransfer.2023.106822
32. Patel P. Exergy and entransy performance analysis of an unmodified 4-stroke CI engine fuelled with CuO, Gr and Al2O3 nano-catalyst-diesel blend at different engine speed. Int J Exergy. 2025;48(1):1-15.
doi:10.1504/IJEX.2025.148554
33. Sundar LS, Singh MK, Ferro MC, Sousa ACM. Experimental investigation of the thermal transport properties of graphene oxide/Co_3O_4 hybrid nanofluids. Int Commun Heat Mass Transf. 2017;84:1-10.
doi: 10.1016/j.icheatmasstransfer.2017.03.001
34. Yadav D, Nirala A, Kumar R, Singh PK. Density variation in nanofluids as a function of concentration and temperature. Mater Today Proc. 2021;46(15):6576-80.
doi: 10.1016/j.matpr.2021.04.052

How to Cite: Mukati M, Maheshwari G. Analysis of Nanofluids in Tube Heat Exchanger. Int Res J Multidiscip Scope. 2026;7(3):1593-1605. DOI: 10.47857/irjms.2026.v07i03.010246